



A review of the ozone hole from 2008 to 2010 as observed by IASI

C. Scannell et al.

A review of the ozone hole from 2008 to 2010 as observed by IASI

**C. Scannell¹, D. Hurtmans², A. Boynard^{1,*}, J. Hadji-Lazaro¹, M. George¹,
A. Delcloo³, O. Tuinder⁴, P.-F. Coheur², and C. Clerbaux^{1,2}**

¹UPMC Univ. Paris 06, CNRS/INSU, UMR8190, LATMOS-IPSL – Université Versailles St.-Quentin, Paris, France

²Spectroscopie de l'Atmosphère, Chimie Quantique et Photophysique, Université Libre de Bruxelles (ULB), Brussels, Belgium

³Royal Meteorological Institute of Belgium, Uccle, Belgium

⁴oyal Netherlands Meteorological Institute, De Bilt, The Netherlands

*now at: Atmospheric Chemistry Division, National Center for Atmospheric Research, Boulder, CO, USA

Received: 23 May 2011 – Accepted: 7 July 2011 – Published: 22 July 2011

Correspondence to: C. Scannell (claire.scannell@gmail.com)

Published by Copernicus Publications on behalf of the European Geosciences Union.

Title Page

Abstract

Introduction

Conclusions

References

Tables

Figures



Back

Close

Full Screen / Esc

Printer-friendly Version

Interactive Discussion



Abstract

Atmospheric remote sensing from satellites is essential for the long-term, continuous monitoring of the ozone hole and is critical in order to evaluate stratospheric ozone recovery. During the last decade, thermal infra-red (TIR) sensors have demonstrated their enhanced capability in capturing both the spatial and temporal variability of the ozone hole during the polar night, in contrast to instruments measuring in the ultraviolet-visible (UV-vis) range of the spectrum which need sunlight to operate. In this paper we present a study of the ozone hole as observed by the Infra-red Atmospheric Sounding Interferometer (IASI) on-board the MetOp-A European satellite platform from the beginning of data dissemination, August 2008, to the end of December 2010. Here we demonstrate IASI's ability to capture the seasonal characteristics of the ozone hole. We compare IASI ozone total columns and vertical profiles with those of the Global Ozone Monitoring Experiment 2 (GOME-2) (also on-board MetOp-A) and electrochemical concentration cell (ECC) ozone sonde measurements for the ozone hole region and period. The IASI and GOME-2 ozone total columns were found to be in excellent agreement for this region with a correlation coefficient of 0.97, for September, October and November 2009. IASI on average, exhibits a positive bias of approximately 7 % compared to the GOME-2 measurements over the entire ozone hole period. Comparisons between IASI and ozone sonde measurements were also found to be in good agreement with the percentage difference between both ozone profile measurements being less than $\pm 30\%$ over the altitude range of 0–40 km. The vertical structure of the ozone hole is in particular captured remarkably good by IASI.

A review of the ozone hole from 2008 to 2010 as observed by IASI

C. Scannell et al.

Title Page

Abstract

Introduction

Conclusions

References

Tables

Figures



Back

Close

Full Screen / Esc

Printer-friendly Version

Interactive Discussion



1 Introduction

Global monitoring of ozone (O_3) is essential as it plays an important role in the chemical processes occurring in the atmosphere and has a major impact on the climate. In the troposphere ozone is considered to be one of the primary air pollutants and main greenhouse gases and in high pollution areas it has been shown to have significant negative impacts on human health and local ecosystems (Slaper et al., 1996). In the stratosphere however, where ozone concentrations greatly exceed those of the troposphere, ozone works to protect the Earth by absorbing the sun's harmful ultraviolet (UV) radiation.

Since the mid 1980s a noticeable severe depletion of stratospheric ozone (reducing to less than 100 DU (= Dobson Units) compared to the average stratospheric ozone concentration of ~300 DU outside of the ozone hole period) has been observed annually over the Antarctic region during the polar springtime (August, September, October and November). Studies into the distribution and evolution of this ozone hole have established that during this period the ozone hole extends over the Antarctic region and increases the level of UV radiation reaching the Earth's surface in the ozone hole region (Newman et al., 2007). This in turn leads to adverse impacts on human health in parts of Australia and South America due to their close proximity to the Antarctic ozone hole (de Laat et al., 2010; Slaper et al., 1996).

Ozone loss rates are determined by the concentrations of active chlorine, bromine, nitrogen and hydrogen oxides present in the atmosphere. It is thought that approximately 60 % of the ozone destruction is caused by the release of active chlorine and the remainder by the release of bromine, hydrogen and nitrogen (Feng et al., 2005). During the polar night (the period in which the Antarctic is in darkness), a polar vortex forms in the Antarctic, holding the air mass within. The lack of sunlight leads to reduced temperatures in the lower stratosphere (at approximately 50 hPa). When the threshold temperatures of 195 K and 188 K are reached, type 1 and type 2 polar stratospheric clouds (PSCs) can form (Maturilli et al., 2005). Heterogeneous reactions can

AMTD

4, 4717–4752, 2011

A review of the ozone hole from 2008 to 2010 as observed by IASI

C. Scannell et al.

Title Page

Abstract

Introduction

Conclusions

References

Tables

Figures

⏪

⏩

◀

▶

Back

Close

Full Screen / Esc

Printer-friendly Version

Interactive Discussion



take place on the surface of PSCs resulting in the release of active chlorine which is a key element in the catalytic destruction of ozone over the Antarctic when the sun comes back. Furthermore nitric acid (HNO₃), a by-product of the heterogeneous reactions remains within the PSCs, which are lost from the stratosphere via sedimentation.

5 This denitrification process results in the unavailability of NO_x to sequester the active chlorine species.

The Montreal protocol and its amendments were designed to protect the ozone layer by phasing out the production of ozone depleting substances containing chlorine and bromine. At the most recent scientific evaluation of the effects of the treaty it was
10 demonstrated that there is evidence of a decrease in the atmospheric burden of ozone depleting substances and that there are some signs of early stratospheric ozone recovery (WMO, 2010). Thus the monitoring of the Antarctic ozone is critical in order to evaluate the effectiveness of this treaty.

Long-term change and variability in ozone levels in the Antarctic have been recorded
15 from several ground based monitoring stations since the discovery of the ozone hole in the 1980s (Fortuin and Kelder, 1998; Balis et al., 2003). These in-situ measurements however are limited both in time and space and though they provide a clear picture of ozone profiles in the Antarctic they fail to offer a complete picture of the temporal and spatial evolution of the ozone hole. Satellite measurements can complement these
20 existing in-situ measurements by providing a unique perspective from which to view the ozone hole, having the capability of providing daily, long term measurements. Current ozone depletion monitoring relies on UV-vis instruments onboard satellites such as TOMS (Total Ozone Mapping Spectrometer), GOME (Global Ozone Monitoring Experiment) and OMI (Ozone Monitoring Instrument), (McPeters and Labow, 1996; Van Roozendaal et al., 2006; Liu et al., 2010). Such instruments while revolutionizing the
25 observation of the extent and depth of the ozone depletion are limited in that many have coarse spatial resolution and that night time retrievals cannot be obtained. No “dark time” measurements is a severe limitation for UV-vis instruments when it comes to the monitoring of the ozone hole as the vortex forms during the Antarctic polar night. As

A review of the ozone hole from 2008 to 2010 as observed by IASI

C. Scannell et al.

Title Page

Abstract

Introduction

Conclusions

References

Tables

Figures

⏪

⏩

◀

▶

Back

Close

Full Screen / Esc

Printer-friendly Version

Interactive Discussion



a result these instruments have large data gaps which can be filled using assimilated data.

The advent of thermal infrared (TIR) sounders such as IASI (Infrared Atmospheric Sounding Interferometer) onboard MetOp-A complements the available datasets, with the advantage that both day and night time measurements are available at high spatial resolution with a small footprint. Here we present a comprehensive study of the ozone hole as viewed by IASI since the beginning of its operation and data dissemination (2008, 2009 and 2010). After a description of the instrument characteristics and the retrieval process (Sect. 2), a detailed description of the Antarctic ozone hole as observed by IASI is provided (Sect. 3). In Sects. 4 and 5 we then evaluate the IASI ozone total column and profile observations along with GOME-2 (which is also onboard the MetOp-A satellite platform) data and in-situ measurements from ground based stations.

2 Ozone retrievals from IASI spectra

2.1 The IASI instrument

The IASI instrument is a high resolution, nadir viewing Fourier transform spectrometer measuring in the thermal infrared part of the spectrum, between 645 and 2760 cm^{-1} . It was launched on board the sun synchronous polar orbiting MetOp-A satellite platform with 2 circular pixels each with a ground footprint of 12 km at the nadir and it has an across track scan with a swath width of 2200 km . It is characterized by a spectral resolution of 0.5 cm^{-1} (apodized) and a spectral sampling of 0.25 cm^{-1} . Depending on the surface temperature and spectral range the retrieved spectra have low radiometric noise estimated to be within the $0.1\text{--}0.4\text{ K}$ and around 0.2 K in the ozone $10\text{ }\mu\text{m}$ region. Due to its large spatial coverage, combined with its low radiometric noise IASI provides twice daily global measurements of key atmospheric species enabling the analysis of species concentrations, global distribution and transport such as O_3 (Boynard et al., 2009) and

A review of the ozone hole from 2008 to 2010 as observed by IASI

C. Scannell et al.

Title Page

Abstract

Introduction

Conclusions

References

Tables

Figures

⏪

⏩

◀

▶

Back

Close

Full Screen / Esc

Printer-friendly Version

Interactive Discussion



A review of the ozone hole from 2008 to 2010 as observed by IASI

C. Scannell et al.

[Title Page](#)[Abstract](#)[Introduction](#)[Conclusions](#)[References](#)[Tables](#)[Figures](#)[Back](#)[Close](#)[Full Screen / Esc](#)[Printer-friendly Version](#)[Interactive Discussion](#)

HNO₃ (Wespes et al., 2009). Other reactive species which are retrieved include carbon monoxide (CO) (George et al., 2009; Pommier et al., 2010), methane (CH₄) (Razavi et al., 2009), sulphur dioxide (SO₂) (Clarisse et al., 2008), ammonia (NH₃) (Clarisse et al., 2009), methanol (CH₃OH) and formic acid (HCOOH) (Coheur et al., 2009; Razavi et al., 2010). For a full detailed overview of the IASI instrument, its specifications and trace gas species that can be retrieved (see Clerbaux et al., 2009).

The IASI mission delivers approximately 1.3×10^6 spectra per day, which are disseminated via Eumetcast, the EUMETSAT data distribution system, 3 h after observation. The absorption lines contained within each spectra are related to the trace gas concentrations via a non linear function of characteristics at the point of measurement such as surface emissivity, temperature profile, other atmospheric components which may interfere with the signal (other trace gases, clouds, aerosols, etc.) and also the characteristics of the instrument itself (spectral resolution, footprint, radiometric noise). To retrieve information about specific atmospheric trace gases from these spectra an inversion algorithm/retrieval scheme needs to be applied.

Figure 1 shows part of the intense (high absorbing) ozone band around 9.6 μm used for retrievals. The black and red spectra represent the observed and fitted IASI spectra respectively. Both spectra clearly portray the characteristic lines in the spectrum associated with ozone absorption in this spectral window (960–1075 cm⁻¹). The grey line shows the residual of the fit which is the difference between what is observed and what is fitted, compared to the instrument noise level (dashed line) in this spectral range. From these spectra we retrieve both columns (total and partial) and profiles from 0–40 km in altitude. Retrievals are performed for scenes with cloud coverage of less than 13 %, using the EUMESAT operational level 2 cloud coverage information, temperature and humidity profiles.

2.2 IASI ozone retrievals

The challenge in developing an ozone retrieval scheme is that it should enable the fast delivery of a global near real time product from the more than 1.3 million IASI

A review of the ozone hole from 2008 to 2010 as observed by IASI

C. Scannell et al.

Title Page

Abstract

Introduction

Conclusions

References

Tables

Figures

⏪

⏩

◀

▶

Back

Close

Full Screen / Esc

Printer-friendly Version

Interactive Discussion



observations per day which are disseminated via the Eumetcast antenna system. In a previous study (Boynard et al., 2009), systematic retrievals of ozone total columns were performed using an algorithm based on the Neural Network (NN) technique (Turquety et al., 2004). For the early stage IASI processing only measurements with a scan angle below 32° on either side of the nadir was considered, and specific issues were identified over icy and sandy surfaces due to the difficulty to properly train the network with insufficient knowledge of the actual emissivity. This while providing a good global overview of the distributions and concentrations of ozone, made it difficult to focus on particular locations such as the Antarctic as not only were there large gaps between each overpass due to the narrow scan angle but also data gaps at the poles, particularly in the southern hemisphere. The Boynard et al. (2009) study found that in general IASI ozone total columns were in good agreement with both GOME-2 and with the Brewer and Dobson ground based instruments with correlation coefficients of 0.9 and 0.85 respectively. This study also found that IASI had a positive bias of about 3.3 % when compared to both GOME-2 and the ozone sondes measurements.

In order to allow the processing of more IASI data at any location the FORLI (Fast Optimal Retrievals on Layers for IASI) O_3 retrieval code was developed at the Université Libre de Bruxelles (ULB) to continuously retrieve ozone profiles from the IASI radiance spectra. Figure 2 shows an Antarctic projection of ozone total column distributions averaged over 3 days at the peak of the 2009 ozone hole (4–6 September), retrieved from the NN scheme and from the FORLI- O_3 scheme. It clearly highlights the improved capability of IASI to capture the spatial variability of total ozone columns in the Antarctic region when using the FORLI- O_3 scheme. The FORLI scheme unlike the initially developed NN scheme has no limit on scan angle width and can adjust the surface temperature and thus processes all the data resulting in a much greater spatial coverage.

For the forward (radiative transfer) model, the code uses pre-calculated look up tables (LUTs) of absorbance at various pressures and temperatures in the spectral region of the ozone band, ($960\text{--}1075\text{ cm}^{-1}$ spectral region, see Fig. 1). LUTs greatly

A review of the ozone hole from 2008 to 2010 as observed by IASI

C. Scannell et al.

Title Page

Abstract

Introduction

Conclusions

References

Tables

Figures

◀

▶

◀

▶

Back

Close

Full Screen / Esc

Printer-friendly Version

Interactive Discussion



minimize the computational time necessary for the retrieval of such a huge quantity of data. These tables are pre-computed on a logarithmic grid for pressure (4.5×10^{-5} – 1 atm) and on a linear grid for temperature (162.8 K–322.64 K) and relative humidity for the water vapour table, using the HITRAN databases (Rothman et al., 2005 and 2009).

5 The Level 2 temperature data distributed by the Eumetcast system are used as input of the code as well as surface emissivity from the MODIS/TERRA or IASI climatology depending on the version of FORLI which is used (Wan, 2008).

The inverse (retrieval) scheme is based on the Optimal Estimation Method (OEM) (Rodgers, 2000) and was developed for the retrieval of ozone profiles from high resolution nadir infrared radiances (e.g. Coheur et al., 2005). This method gives the optimal solution for a state vector x (in this case the O_3 profile), for given a measurement y , the IASI radiance spectra, with an error covariance S_ε and the equation $y = F(x, b) + \varepsilon$, where F is the forward radiative transfer model, b represents the model parameters affecting the measurement and ε is the measurement noise.

15 Solving such a problem is complex as there can be many solutions which fit the observations. Therefore to find a meaningful solution it is necessary to constrain the results with some a priori information, x_a the a priori profile that represents the expected average profile and S_a the covariance matrix that ideally represents the true variability of the species about the average. The solution can be found by iteratively applying:

$$20 \hat{x}_{i+1} = x_a + D_y [y - F(\hat{x}_i) - K_i (x_a - \hat{x}_i)] \quad (1)$$

with $D_y = \hat{S}_i K_i^T S_\varepsilon^{-1}$ and $\hat{S}_{i+1} = (K_{i+1}^T S_\varepsilon^{-1} K_{i+1} + S_a^{-1})^{-1}$ where $K_i = (\frac{\partial F}{\partial x})_i$ is the Jacobian at state x_i , K_i^T is its transpose and \hat{x}_{i+1} is the new state vector. The matrix D_y is the matrix of contribution factors and the error covariance of the solution is given by \hat{S}_{i+1} . The iteration starts with some initial estimate of the state, the a priori information x_a , and the covariance matrix S_a , and terminates when convergence is reached.

25 The choice of a priori information is an important factor for the construction of the retrievals in the infr-red. Here the a priori profile and associated covariance matrix, were constructed using the Logan/Labow/McPeters climatological database (McPeters et al.,

is observed, it is weaker and the absorption lines seem to disappear due to the combined absorption and emission in the atmospheric layers (due to specific temperature conditions).

A global distribution of the DOFs and the averaging kernels associated with each of these spectra are depicted in Fig. 4. This figure highlights the difficulties in retrieving ozone concentrations over the Antarctic region. As previously discussed, the DOFs are a measure of the vertical sensitivity of the measurement, i.e. the higher the number of DOFs the more vertical layers can be discriminate. Figure 4 (left panel) shows that over the ocean, the DOFs generally range between 3 and 4, while over the ice caps the DOFs range between 1 and 2. Because of the weaker signal over the ice, part of the vertical information is lost. These results indicate that care is needed when selecting spectra over the Antarctic land mass. As shown in Fig. 4 (middle), the averaging kernels associated with the measurement over the ocean are well defined, with DOFs of 3.3, while those associated with the measurement taken over the ice (Fig. 4, right panel) can appear ill formed, with DOFs of less than 1.5.

The ozone hole area is defined as the region of ozone located south of 40° S and where ozone values fall below the threshold value of 220 DU (WMO, 2002). Recent studies have shown that during the 1980s the ozone hole over Antarctica expanded rapidly, this expansion slowed in the 1990s and in the last few years this expansion and ozone loss rates have appeared to level out but also the ozone loss rates (Newman et al., 2006, 2009).

Figure 5 shows an example of typical ozone maps over the Antarctic during the ozone hole period. The maps plot the weekly averaged IASI ozone total columns on a 1° × 1° grid for the September of 2008, 2009 and 2010. This period marks the time when the ozone hole area is at its largest and when ozone loss for this region is at its greatest. Such distribution maps show that the size, shape and evolution of both the hole, its vortex and the ozone concentrations of both can be clearly monitored.

Figure 6 depicts a time series of the daily temporal evolution of IASI total ozone concentrations (black lines), retrieved from FORLI-O3 and averaged over 5° latitude bands

A review of the ozone hole from 2008 to 2010 as observed by IASI

C. Scannell et al.

Title Page

Abstract

Introduction

Conclusions

References

Tables

Figures



Back

Close

Full Screen / Esc

Printer-friendly Version

Interactive Discussion



from 50° S to 90° S, from the beginning of August 2008 to the end of December. It is worth noting here that FORLI-O3 algorithm has been upgraded several times since its development and as such this data set was obtained using slightly different versions of the algorithm. The shaded grey area represents the standard deviation ($\pm\sigma$) about this average. Apart from a few spurious points, the spread of the data is minimal for all periods outside the ozone hole phase. The highlighted blue area represents the ozone hole period, August to December of each year. This figure clearly illustrates the seasonal cycle of ozone reduction over the Antarctic during the polar spring, beginning at the end of August and finishing by the end of November. For all years distinct features exist. One such feature is that the ozone hole itself forms annually south of 60° S. Another is that north of 60° S there is a noticeable rise in ozone concentrations during the ozone hole periods which are representative of the edge of the vortex surrounding the ozone hole. Moving southwards it is also evident that the decrease in ozone concentrations and the longevity of the hole itself become more pronounced. Each year the peak of the ozone hole occurs by mid September and at this time ozone concentrations are seen to decrease by more than 50 % below 75° S to approximately 150 DU.

Despite these well observed trends there are some inter-annual variations. In 2009 there was a sharp increase in ozone concentrations in mid October (circled areas) that is not visible in 2008 or 2010. Figure 7 illustrates how during this period the polar vortex became more elliptical in shape. This lead to the early depletion of polar stratospheric clouds in some regions that were previously within the vortex, as they became exposed to sunlight resulting in the increase in ozone concentrations (British Antarctic Survey, 2010). By 22 October the polar vortex had reverted back to the more standard circular rotation reducing ozone concentrations within the hole to levels similar to those prior to its elliptical circulation. In 2010 there was a relatively slow start to the ozone hole formation (the beginning of September as opposed to mid August) in comparison with other years (see Fig. 6). This was due mainly to higher than average temperatures in the stratosphere over the Antarctic resulting in the reduction in the volume of polar stratospheric clouds in mid to late August of this year. Also in 2010 the ozone hole

A review of the ozone hole from 2008 to 2010 as observed by IASI

C. Scannell et al.

[Title Page](#)[Abstract](#)[Introduction](#)[Conclusions](#)[References](#)[Tables](#)[Figures](#)[◀](#)[▶](#)[◀](#)[▶](#)[Back](#)[Close](#)[Full Screen / Esc](#)[Printer-friendly Version](#)[Interactive Discussion](#)

period extended into late December with ozone values not rising above the 220 DU threshold limit until 21 December. For this 3 year study the ozone hole area was at its largest for this time of the year.

Figure 8 (solid lines) illustrates the temporal evolution of the ozone hole area from August to the end of December for 2008 (green), 2009 (blue) and 2010 (red). It is compiled from weekly averaged area values of the ozone hole from $1^\circ \times 1^\circ$ grid resolution data sets. Of the 3 years studied 2008 (green) proved to be the severest ozone hole period, beginning in mid August and lasting until the beginning of December. The maximum hole area occurred at the end of September and reached values of more than 25 million square kilometers. In 2009 the ozone hole (blue) had a shorter lifetime than 2008 and was less severe, beginning again in mid August and dissipating by the end of November. In September the ozone hole area was at its greatest with an area size of approximately 24 million square kilometers. For 2010 (red) the ozone hole area expansion began in the beginning of September, much later than previous years and its maximum area reached a value of 21 million square kilometers. However despite 2010 being less severe, its area declined less rapidly than in the previous years with the ozone hole period extending into late December before dissipating off.

4 Comparison with GOME-2 ozone total columns

As previously discussed, the UV-vis instrument GOME-2 is also on board the MetOp-A platform. In this section we compare IASI and GOME-2 ozone total column retrievals during the Antarctic ozone hole. GOME-2 is a UV-vis, cross track, nadir viewing spectrometer working in the 240–790 nm spectral range. It has a default field of view of 80×40 km, which may be varied to the smaller field of view of 5×40 km and it has a swath width of approximately 1920 km providing almost daily coverage at the equator. The GOME-2 total ozone column is calculated as a vertically integrated ozone profile based on the vertical ozone profile retrieval algorithm OPERA developed and run operationally in near real time by KNMI in the framework of the EUMETSAT O3MSAF.

A review of the ozone hole from 2008 to 2010 as observed by IASI

C. Scannell et al.

Title Page

Abstract

Introduction

Conclusions

References

Tables

Figures



Back

Close

Full Screen / Esc

Printer-friendly Version

Interactive Discussion



For this study both IASI and GOME-2 total column ozone distributions were averaged to a $1^\circ \times 1^\circ$ grid. As the GOME-2 measurements are not available during some of the polar night, IASI observations during this period without sunlight were excluded from the following analysis.

The ozone hole as observed from GOME-2 for 2008–2010 is presented in Fig. 8. It is clear that in general IASI and GOME-2 compare quite well, observing similar peaks and similar beginning and end periods during these 3 years. GOME-2 however did measure a marginally larger ozone hole for all 3 years with the maximum difference of 7.5 % measured between the two instruments in 2008.

Figure 9 shows the averaged monthly distributions of total ozone in DU for both IASI and GOME-2 (first and second columns respectively) over the Antarctic region for the ozone hole season, August through to November 2009. Despite the effect of GOME-2 being unable to measure completely during the polar night, which is visible from the data gaps at the centre of the Antarctic for August and September, both instruments show similar structures for the ozone total columns. As expected for each month maximum total ozone is observed in the polar vortex and minimum total ozone is observed within the ozone hole. The temporal and spatial evolution of the ozone hole throughout the period is also well observed by both instruments. It is worth noting for August and September the data gaps visible in the GOME-2 data set can be filled using assimilated data and for October and November sufficient light is available so that almost full retrievals from GOME-2 are possible.

The third column in Fig. 9 presents the percentage difference between IASI and GOME-2. Despite both instruments observing similar structures for all months, IASI in general measures between 5 %–10 % higher ozone concentrations and observes a much stronger vortex surrounding the ozone hole than GOME-2. The predominant difference occurs during the August and September periods where IASI has a positive bias of between 20 %–30 % surrounding the ozone hole core, where for these periods GOME-2 measures a larger decrease in the ozone concentrations than IASI within the ozone hole itself. In November there is a negative bias within the hole area as

A review of the ozone hole from 2008 to 2010 as observed by IASI

C. Scannell et al.

Title Page

Abstract Introduction

Conclusions References

Tables Figures

⏪ ⏩

◀ ▶

Back Close

Full Screen / Esc

Printer-friendly Version

Interactive Discussion

Discussion Paper | Discussion Paper | Discussion Paper | Discussion Paper | Discussion Paper



A review of the ozone hole from 2008 to 2010 as observed by IASI

C. Scannell et al.

Title Page

Abstract

Introduction

Conclusions

References

Tables

Figures

⏪

⏩

◀

▶

Back

Close

Full Screen / Esc

Printer-friendly Version

Interactive Discussion



IASI measures a slightly larger elongated ozone hole than GOME-2. In the vortex for all months a positive bias of approximately 7/8% is also observed as IASI measures larger concentrations than GOME-2. However in general the difference between the two instruments remains below 10%. Previous studies have shown such a bias (of approximately 5%) exists between TIR and UV-vis observations and may be due to discrepancies of spectroscopic parameters such as differences in the absorption cross section and line parameters (e.g. Schneider et al., 2008; Anton, 2011). A recent study by Massart et al. (2009), also found that IASI tends to overestimate the ozone total columns in comparison to a model forced by the total columns retrieved from MLS (microwave limb sounder) and SCIAMACHY (Scanning Imaging Absorption spectrometer for Atmospheric Cartography).

Figure 10 presents a statistical comparison between IASI and GOME-2 ozone total columns that was performed for September, October and November of 2009. The correlation coefficients and the bias about the mean are inset into the graph for each month. The black data below 220 DU and above 320 DU represent ozone values within the ozone hole and in its associated vortex respectively. The grey data represents all other data south of 45° S, the area for which the ozone hole is defined, which do not lie within the hole or vortex regions. The linear regression for each month (solid red lines), the confidence intervals (dashed red lines) and the 1:1 ratio reference line (dashed green line) are also presented in the figure. It is clear from the strong correlation coefficients for each month ($r^2 = 0.967$, $r^2 = 0.973$ and $r^2 = 0.975$) that IASI and GOME-2 are closely comparable throughout the entire ozone hole region and period. Based on these regression lines IASI shows a slight positive bias as previously highlighted by the relative difference plots.

At the ozone hole region both instruments compare quite well, though slight differences in the measurement of the ozone hole size and shape by IASI and GOME-2 gives rise to some spurious data points in this region. This is particularly the case in October and November where GOME-2 measures some higher ozone concentrations than IASI in the ozone hole. Though as already discussed there is an identified bias

between the two instruments and efforts should be made to fully understand this, some differences between the instruments can be attributed to the different modes of observation which have not been accounted for in this analysis. For example both instruments have a different ground footprint and observation geometry and thus are subject to different cloud contamination and probe different air masses. Both instruments also have different vertical sensitivities, IASI has a maximum sensitivity to the ozone profile in the upper troposphere–lower stratosphere while GOME-2 has a maximum sensitivity in the stratosphere.

5 Comparison with ozone sondes

The in-situ ozone-sonde profile measurements used in this study are from the WOUDC (World Ozone and Ultra Violet Radiation Data Centre) data base and the location of each indicated in figure 11 are the German Neumayer station (78°39' S; 08°15' W, WMO no. 323), the Australian Davis station (68°35' S; 77°58' E, WMO no. 450) and the Argentinian USH station (54°88' S; 68°19' W, WMO no. 339) in blue, red and green respectively. Each station is equipped with electrochemical concentration cell (ECC) ozone-sondes which utilize the oxidation reaction of ozone with potassium iodide to determine the ozone concentration throughout the profile. These ozone-sondes measure the profile of ozone up to 30 km into the atmosphere.

It should be noted that over this particular region finding a collocation between IASI, GOME-2 and an ozone sonde was not possible because ozone sonde measurements are not daily and GOME-2 due to its geometry may be scanning a different location to IASI and the ozone sonde. The primary challenge with comparing IASI and ozone sonde measurements is the relatively small number of co-incident measurements between satellite and sondes in the Antarctic. A set of strict co-occurrence criteria were applied so as to correctly compare the IASI retrieved ozone profiles with the in-situ ozone profiles. Only those measurements that were co-located in space to within 0.5°

A review of the ozone hole from 2008 to 2010 as observed by IASI

C. Scannell et al.

Title Page

Abstract

Introduction

Conclusions

References

Tables

Figures

⏪

⏩

◀

▶

Back

Close

Full Screen / Esc

Printer-friendly Version

Interactive Discussion



and co-located in time to within 6 h were chosen. For the cases where 2 or more such IASI profiles fit the co-locations an averaged profile was calculated for the comparison.

Secondly to make comparisons between IASI and the ozone-sondes, the difference in vertical resolution and sensitivity between the two data sets must be accounted for.

For this reason the IASI averaging kernel and constraints are applied to the ozone-sonde data following Eq. (2), producing a vertical profile that represents what IASI would measure for the same air sampled by the sonde. For a more in-depth description of this method see Rodgers (2000).

Finally it should be noted that the sonde data are supplied in units of ozone partial pressure on a vertical scale of atmospheric pressure while the IASI data are supplied in molecules cm^{-3} on a vertical scale of atmospheric height. Therefore before the ozone-sonde data can be convolved with the IASI averaging kernels, the vertical scales and the units must be homogenized via a simple extrapolation and unit conversion as follows:

$$n = 10^{-9} \frac{P_{\text{part}}}{kT} \quad (3)$$

where n is in molecules cm^{-3} , P_{part} is ozone in partial pressure in hPa, k is the Boltzmann constant ($1.3807 \times 10^{-23} \text{ JK}^{-1} \text{ molecule}^{-1}$) and T is the temperature in K.

Figure 12 shows an example of a IASI and ozone-sonde profiles (red and blue profiles respectively) taken from within the ozone hole during September 2009. The IASI a priori profile (dotted black profile) is also represented for each location. As previously discussed in Sect. 2.2 retrieving ozone profiles with IASI over the ice can prove difficult thus it should be noted that the averaging kernels for each collocation between IASI and the ozone-sonde were closely studied and only those measurements with well defined averaging kernels and DOFs greater than or equal to 3 were chosen for this comparison.

In the ozone hole region IASI is seen to be very sensitive in shape and magnitude to the profiles measured by the ozone sonde. The same features are observed by both

A review of the ozone hole from 2008 to 2010 as observed by IASI

C. Scannell et al.

Title Page

Abstract

Introduction

Conclusions

References

Tables

Figures

⏪

⏩

◀

▶

Back

Close

Full Screen / Esc

Printer-friendly Version

Interactive Discussion



instruments such as the notable decrease in ozone concentrations between 15–20 km, however IASI does over estimate slightly in the lower troposphere for all cases.

In the vortex (Fig. 13) for the USH and Davis stations IASI compares well to the convolved ozone sondes with only marginal differences in shape and magnitude. In the troposphere there is almost no difference while in the stratosphere IASI slightly over estimates in comparison to the USH station and under estimates for the Davis station. A percentage difference calculation between the IASI and the convolved sonde ozone profiles for each station found that IASI and the sondes compare to within 20 % and within 30 % for the other two cases and demonstrates just how accurately IASI can estimate the shape and size of ozone profiles during the ozone hole period.

6 Summary and conclusion

This paper presents an assessment of the capabilities of IASI to perform continuous, precise measurements of the ozone hole. IASI will fly continuously for the next 10 years (on MetOp-B and -C), which should be followed by an improved IASI instrument in the 2019 timeframe. As already reported for CO in Pommier et al. (2010), polar regions are at the same time easy to observe as they are well covered by the MetOp polar orbiting satellite, but on the other hand difficult to process due to the specific low temperature and thermal contrast conditions and frozen surfaces that impact the radiance spectra. In this work, the FORLI-O3 retrieval scheme was utilized. This retrieval algorithm allows the processing of global distributions of ozone two times per day, in near real time, from all the IASI spectra with cloud contamination of less than 13 %.

In this work we analyze the IASI ozone total columns distributions over the Antarctic to study the ozone hole evolution in 2008, 2009 and 2010. Our results highlight the capability of IASI to capture very precisely the short term spatial and temporal variability of the ozone hole development, including during the polar night. Data comparisons between IASI and GOME-2 observations of the ozone total column were performed for the three ozone hole periods and showed excellent agreement for both the timing

A review of the ozone hole from 2008 to 2010 as observed by IASI

C. Scannell et al.

Title Page

Abstract

Introduction

Conclusions

References

Tables

Figures

⏪

⏩

◀

▶

Back

Close

Full Screen / Esc

Printer-friendly Version

Interactive Discussion



A review of the ozone hole from 2008 to 2010 as observed by IASI

C. Scannell et al.

Title Page

Abstract

Introduction

Conclusions

References

Tables

Figures

⏪

⏩

◀

▶

Back

Close

Full Screen / Esc

Printer-friendly Version

Interactive Discussion



and size of the hole. A detailed comparison for 2009 provided correlation coefficients of 0.97 for September, October and November. For this region IASI showed an average positive bias of approximately 7%. This is in keeping with previous research by Boynard et al. (2009) who found an average positive bias of between 3%–5% on a global scale.

The retrieval of ozone vertical profiles from IASI spectra collocated with ozone sonde measurements for September 2009 was also performed. Here we found that IASI showed good agreement with the sonde measurements from the troposphere to the stratosphere, with the difference between IASI and the sondes being less than 30% within the hole itself. IASI was also found to be very sensitive to the ozone profile in the lower stratosphere between 15–20 km, remarkably capturing the vertical extent of the ozone hole, as shown by the good agreement with the ozone sondes.

Such continuous IASI ozone measurements are complementing existing data in the long term trend assessment of ozone which suggests that the ozone hole expansion and ozone loss rates have appeared to have stopped (WMO, 2010).

Work is in progress to combine the IASI and GOME-2 profile products to derive improved profiles. Theoretical studies have shown that improvements in measuring the troposphere could be achieved via the combination of complimentary UV and TIR measurements (Zhang et al., 2010; Worden et al., 2007). This study is a first step in identifying the potential difficulties encountered when dealing with real observations.

Acknowledgements. IASI has been developed and built under the responsibility of the Centre National des Etudes Spatiales (CNES, France). It is flown onboard the MetOp satellites as part of the EUMETSAT Polar System. The IASI level 1 data are distributed in near real time by EUMETSAT through the Eumetcast dissemination system. The authors acknowledge the Ether French atmospheric database (<http://ether.ipsl.jussieu.fr>) for providing the IASI data. The GOME-2 level 2 data were provided by the DLR and KNMI through Eumetcast. These data were generated under the auspices of the O3M SAF project of EUMETSAT. The ozone sonde data used in this work were provided by the World Ozone and Ultraviolet Data Centre (WOUDC), the Southern Hemisphere Additional Ozone sondes (SHADOZ) and the Global Monitoring Division (GMD) of NOAA's Earth System Research Laboratory

and are publically available (<http://www.woudc.org>, <http://croc.gsfc.nasa.gov/shadoz> and <http://www.esrl.noaa.gov/gmd>). All the agencies cited above are acknowledged for providing data. The research in France was conducted with the financial support of CNES. The research in Belgium was funded by the “Actions de Recherche Concertées” (Communauté Française), the Fonds National de la Recherche Scientifique (FRS-FNRS F.4511.08), the Belgian State Federal Office for Scientific, Technical and Cultural Affairs and the European Space Agency (EAS-Prodex C90-327).



The publication of this article is financed by CNRS-INSU.

References

- Antón, M., Loyola, D., Clerbaux, C., López, M., Vilaplana, J. M., Bañón, M., Hadji-Lazaro, J., Valks, P., Hao, N., Zimmer, W., Coheur, P. F., Hurtmans, D., and Alados-Arboledas, L.: Validation of the Metop-A total ozone data from GOME-2 and IASI using reference ground-based measurements at the Iberian Peninsula, *Remote Sens. Environ.*, 115, 1380–1386, 2011.
- Balis, D. S. and Bojkov, R. D. : Characteristics of Antarctic Spring ozone decline from satellite and ground based measurements from the appearance of the “ozone hole” up to December 2001, edited by: Harris, N., Amanatidis, G., and Levine, J., *Europ. Com. Air Pollution Research Report No. 79*, Proc. of the 6th Europ. Symp. on Stratospheric Ozone in Goeteborg, Sweden, 39–42, 2003.
- Boynard, A., Clerbaux, C., Coheur, P.-F., Hurtmans, D., Turquety, S., George, M., Hadji-Lazaro, J., Keim, C., and Meyer-Arneke, J.: Measurements of total and tropospheric ozone from IASI: comparison with correlative satellite, ground-based and ozonesonde observations, *Atmos. Chem. Phys.*, 9, 6255–6271, doi:10.5194/acp-9-6255-2009, 2009.

A review of the ozone hole from 2008 to 2010 as observed by IASI

C. Scannell et al.

Title Page

Abstract

Introduction

Conclusions

References

Tables

Figures



Back

Close

Full Screen / Esc

Printer-friendly Version

Interactive Discussion



A review of the ozone hole from 2008 to 2010 as observed by IASI

C. Scannell et al.

Title Page

Abstract

Introduction

Conclusions

References

Tables

Figures

◀

▶

◀

▶

Back

Close

Full Screen / Esc

Printer-friendly Version

Interactive Discussion



- British Antarctic Survey: Ozone bulletin, <http://www.theozonehole.com/2010ozone.htm>, last access: July 2011, The Ozone Hole, 2010.
- Clarisse, L., Coheur, P. F., Prata, A. J., Hurtmans, D., Razavi, A., Phulpin, T., Hadji-Lazaro, J., and Clerbaux, C.: Tracking and quantifying volcanic SO₂ with IASI, the September 2007 eruption at Jebel at Tair, *Atmos. Chem. Phys.*, 8, 7723–7734, doi:10.5194/acp-8-7723-2008, 2008.
- Clarisse, L., Clerbaux, C., Dentener, F., Hurtmans, D., and Coheur, P-F.: Global ammonia distribution derived from infrared satellite observations, *Nat. Geosci.*, 2, 479–483, doi:10.1038/NGEO551, 2009.
- Clerbaux, C., Boynard, A., Clarisse, L., George, M., Hadji-Lazaro, J., Herbin, H., Hurtmans, D., Pommier, M., Razavi, A., Turquety, S., Wespes, C., and Coheur, P-F.: Monitoring of atmospheric composition using the thermal infrared IASI/MetOp sounder, *Atmos. Chem. Phys.*, 9, 6041–6054, doi:10.5194/acp-9-6041-2009, 2009.
- Coheur, P-F., Barret, B., Turquety, S., Hurtmans, D., Hadji-Lazaro, J., and Clerbaux, C.: Retrieval and characterization of ozone vertical profiles from a thermal infrared nadir sounder, *J. Geophys. Res.*, 110, D24303, doi:10.1029/2005JD005845, 2005.
- Coheur, P-F., Clarisse, L., Turquety, S., Hurtmans, D., and Clerbaux, C.: IASI measurements of reactive trace species in biomass burning plumes, *Atmos. Chem. Phys.*, 9, 5655–5667, doi:10.5194/acp-9-5655-2009, 2009.
- De Laat, A. T. J., van der A, R. J., Allaart, M. A. F., van Weele, M., Benitez, G. C., Casaccia, C., Paes Leme, N. M., Quel, E., Salvador, J., and Wolfram, E. : Extreme sunbathing: Three weeks of small total O₃ columns and high UV radiation over the southern tip of South America during the 2009 Antarctic O₃ hole season, *Geophys. Res. Lett.*, 37, L14805, doi:10.1029/2010GL043699, 2010.
- Feng, W., Chipperfield, M. P., Davies, S., Sen, B., Toon, G., Blavier, J. F., Webster, C. R., Volk, C. M., Ulanovsky, A., Ravegnani, F., von der Gathen, P., Jost, H., Richard, E. C., and Claude, H.: Three-dimensional model study of the Arctic ozone loss in 2002/2003 and comparison with 1999/2000 and 2003/2004, *Atmos. Chem. Phys.*, 5, 139–152, doi:10.5194/acp-5-139-2005, 2005.
- Fortuin, J. P. F. and Kelder, H.: An ozone climatology based on ozone sonde and satellite measurements, *J. Geophys. Res.*, 103, 31709–31734, 1998.

A review of the ozone hole from 2008 to 2010 as observed by IASI

C. Scannell et al.

Title Page

Abstract

Introduction

Conclusions

References

Tables

Figures

◀

▶

◀

▶

Back

Close

Full Screen / Esc

Printer-friendly Version

Interactive Discussion



George, M., Clerbaux, C., Hurtmans, D., Turquety, S., Coheur, P.-F., Pommier, M., Hadji-Lazaro, J., Edwards, D. P., Worden, H., Luo, M., Rinsland, C., and McMillan, W.: Carbon monoxide distributions from the IASI/METOP mission: evaluation with other space-borne remote sensors, *Atmos. Chem. Phys.*, 9, 8317–8330, doi:10.5194/acp-9-8317-2009, 2009.

5 Liu, X., Bhartia, P. K., Chance, K., Froidevaux, L., Spurr, R. J. D., and Kurosu, T. P.: Validation of Ozone Monitoring Instrument (OMI) ozone profiles and stratospheric ozone columns with Microwave Limb Sounder (MLS) measurements, *Atmos. Chem. Phys.*, 10, 2539–2549, doi:10.5194/acp-10-2539-2010, 2010.

Massart, S., Clerbaux, C., Cariolle, D., Piacentini, A., Turquety, S., and Hadji-Lazaro, J.: First steps towards the assimilation of IASI ozone data into the MOCAGE-PALM system, *Atmos. Chem. Phys.*, 9, 5073–5091, doi:10.5194/acp-9-5073-2009, 2009.

Maturilli, M., Neuber, R., Massoli, P., Cairo, F., Adriani, A., Moriconi, M. L., and Di Donfrancesco, G.: Differences in Arctic and Antarctic PSC occurrence as observed by lidar in Ny-Ålesund (79° N, 12° E) and McMurdo (78° S, 167° E), *Atmos. Chem. Phys.*, 5, 2081–2090, doi:10.5194/acp-5-2081-2005, 2005.

15 McPeters, R. D. and Labow, G. J.: An assessment of the accuracy of 14.5 years of nimbus 7 TOMS version 7 ozone data by comparison with the Dobson network, *Geophys. Res. Lett.*, 23, 3695–3698, 1996.

McPeters, R. D., Labow, G. J., and Logan, J. A.: Ozone climatological profiles for satellite retrieval algorithms, *J. Geophys. Res.*, 112, D05308, doi:10.1029/2005JD006823, 2007.

Newman, P. A., Nash, E. R., Kawa, S. R., Montzka, S. A., and Schauffler, S. M.: When will the ozone hole recover?, *Geophys. Res. Lett.*, 33, L12814, doi:10.1029/2005GL025232, 2006.

20 Newman, P. A., Rex, M., Canziani, P. O., Carslaw, K. S., Drdla, K., Godin-Beekmann, S., Golden, D. M., Jackman, C. H., Kreher, K., Langematz, U., Müller, R., Nakane, H., Orsolini, Y. J., Salawitch, R. J., Santee, M. L., von Hobe, M., and Holden, S.: Polar Ozone: Past and Present, Chapter 4 in *Scientific Assessment of Ozone Depletion: 2006*, Global Ozone Research and Monitoring Project – Report No. 50, World Meteorological Organization, Geneva, Switzerland, 2007.

30 Newman, P. A., Oman, L. D., Douglass, A. R., Fleming, E. L., Frith, S. M., Hurwitz, M. M., Kawa, S. R., Jackman, C. H., Krotkov, N. A., Nash, E. R., Nielsen, J. E., Pawson, S., Stolarski, R. S., and Velders, G. J. M.: What would have happened to the ozone layer if chlorofluorocarbons (CFCs) had not been regulated?, *Atmos. Chem. Phys.*, 9, 2113–2128, doi:10.5194/acp-9-2113-2009, 2009.

A review of the ozone hole from 2008 to 2010 as observed by IASI

C. Scannell et al.

Title Page

Abstract

Introduction

Conclusions

References

Tables

Figures

◀

▶

◀

▶

Back

Close

Full Screen / Esc

Printer-friendly Version

Interactive Discussion



- Pommier, M., Law, K. S., Clerbaux, C., Turquety, S., Hurtmans, D., Hadji-Lazaro, J., Coheur, P.-F., Schlager, H., Ancellet, G., Paris, J.-D., Nédélec, P., Diskin, G. S., Podolske, J. R., Holloway, J. S., and Bernath, P.: IASI carbon monoxide validation over the Arctic during POLARCAT spring and summer campaigns, *Atmos. Chem. Phys.*, 10, 10655–10678, doi:10.5194/acp-10-10655-2010, 2010.
- Razavi, A., Clerbaux, C., Wespes, C., Clarisse, L., Hurtmans, D., Payan, S., Camy-Peyret, C., and Coheur, P. F.: Characterization of methane retrievals from the IASI space-borne sounder, *Atmos. Chem. Phys.*, 9, 7889–7899, doi:10.5194/acp-9-7889-2009, 2009.
- Razavi, A., Karagulian, F., Clarisse, L., Hurtmans, D., Coheur, P. F., Clerbaux, C., Müller, J. F., and Stavrakou, T.: Global distributions of methanol and formic acid retrieved for the first time from the IASI/MetOp thermal infrared sounder, *Atmos. Chem. Phys.*, 11, 857–872, doi:10.5194/acp-11-857-2011, 2011.
- Rothman, L. S., Jacquemart, D., Barbe, A., Benner, D. C., Birk, M., Brown, L. R., Carleer, M. R., Chackerian Jr., C., Chance, K., Coudert, L. H., Dana, V., Devi, V. M., Flaud, J.-M., Gamache, R. R., Goldman, A., Hartman, J.-M., Jucks, K. W., Maki, A. G., Mandin, J.-Y., Massie, S. T., Orphal, J., Perrin, A., Rinsland, C. P., Smith, M. A. H., Tennyson, J., Tolchenov, R. N., Toth, R. A., Vander Auwera, J., Varanasi, P., and Wagner, G.: The HITRAN 2004 molecular spectroscopic database, *J. Quant. Spectrosc. Ra.*, 96, 139–204, 2005.
- Rothman, L. S., Gordon, I. E., Barbe, A., Benner, D. C., Bernath, P. F., Birk, M., Boudon, V., Brown, L. R., Campargue, A., Champion, J.-P., Chance, K., Coudert, L. H., Dana, V., Devi, V. M., Fally, S., Flaud, J.-M., Gamache, R. R., Goldman, A., Jacquemart, D., Kleiner, I., Lacombe, N., Lafferty, W. J., Mandin, J.-Y., Massie, S. T., Mikhailenko, S. N., Miller, C. E., Moazzen-Ahmadi, N., Naumenko, O., Nikitin, A. V., Orphal, J., Perevalov, V. I., Perrin, A., Predoi-Cross, A., Rinsland, C. P., Rotger, M., Simecková, M., Smith, M. A. H., Sung, K., Tashkun, S. A., Tennyson, J., Toth, R. A., Vandaele, A. C., and Vander Auwera, J.: The HITRAN 2008 molecular spectroscopic database, *J. Quant. Spectrosc. Ra.*, 110, 533–572, 2009.
- Schneider, M., Redondas, A., Hase, F., Guirado, C., Blumenstock, T., and Cuevas, E.: Comparison of ground-based Brewer and FTIR total column O₃ monitoring techniques, *Atmos. Chem. Phys.*, 8, 5535–5550, doi:10.5194/acp-8-5535-2008, 2008.
- Slaper, H., Velders, G. J. M., Daniel, J. S., DeGruijil, F. R., and Van der Leun, J. C.: Estimates of ozone depletion and skin cancer incidence to examine the Vienna Convention achievements, *Nature*, 384, 256–258, 1996.

A review of the ozone hole from 2008 to 2010 as observed by IASI

C. Scannell et al.

[Title Page](#)
[Abstract](#)
[Introduction](#)
[Conclusions](#)
[References](#)
[Tables](#)
[Figures](#)
[Back](#)
[Close](#)
[Full Screen / Esc](#)
[Printer-friendly Version](#)
[Interactive Discussion](#)


- van Roozendael, M., Loyola, D., Spurr, R., Balis, D., Lambert, J. C., Livschitz, Y., Valks, P., Ruppert, T., Kenter, P., Fayt, C., and Zehner, C.: Ten years of GOME/ERS2 total ozone data: the new GOME data processor (GDP) version 4: I. Algorithm description, *J. Geophys. Res.*, 111, D14311, doi:10.1029/2005JD006375, 2006.
- 5 Wan, Z.: New refinements and validation of the MODIS land surface temperature/emissivity products, *Remote Sens. Environ.*, 512, 59–74, 2008.
- Wespes, C., Hurtmans, D., Clerbaux, C., Santee, M. L., Martin, R. V., and Coheur, P. F.: Global distributions of nitric acid from IASI/MetOP measurements, *Atmos. Chem. Phys.*, 9, 7949–7962, doi:10.5194/acp-9-7949-2009, 2009.
- 10 Worden, J., Liu, X., Bowman, K., Chance, K., Beer, R., Eldering, A., Gunson, M., and Worden, H.: Improved tropospheric ozone profile retrievals using OMI and TES radiances, *Geophys. Res. Lett.*, 34, L01809, doi:10.1029/2006GL027806, 2007.
- WMO – World Meteorological Organization: Scientific assessment of ozone depletion, *Global Ozone Res. Monit. Proj.*, Rep. 47, Geneva, Switzerland, 2002.
- 15 WMO – World Meteorological Organization: Nohende Ajavon, A.-L., Newman, P. A., Pyle, J. A., and Ravishankara, A. R. (Assessment cochairs): Scientific assessment of ozone depletion, *Global ozone and research and monitoring project*, Report No. 52, 2010.
- Zhang, L., Jacob, D. J., Liu, X., Logan, J. A., Chance, K., Eldering, A., and Bojkov, B. R.: Intercomparison methods for satellite measurements of atmospheric composition: appli-
 20 cation to tropospheric ozone from TES and OMI, *Atmos. Chem. Phys.*, 10, 4725–4739, doi:10.5194/acp-10-4725-2010, 2010.

A review of the ozone hole from 2008 to 2010 as observed by IASI

C. Scannell et al.

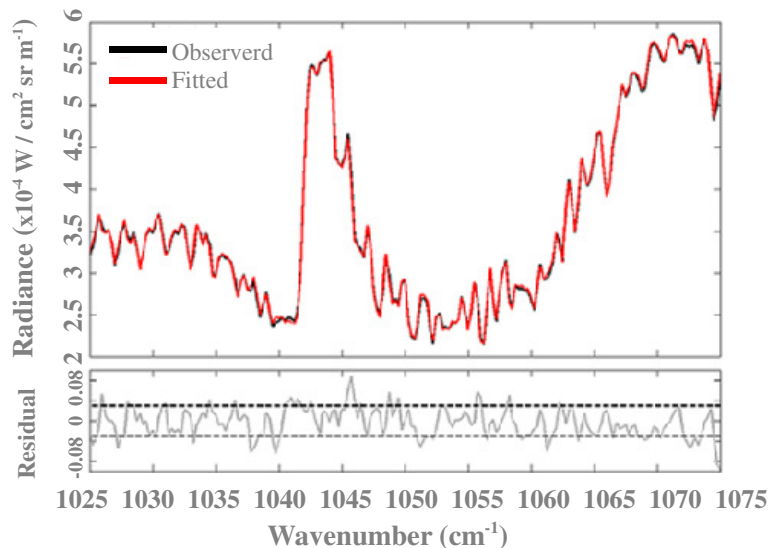


Fig. 1. Example of the intense ozone band region (1025 cm⁻¹–1075 cm⁻¹) of a typical IASI spectrum (observed and calculated using a radiative transfer code). The grey line in represents the residual of the fit which is comparable to the IASI instrument noise level (dashed line).

A review of the ozone hole from 2008 to 2010 as observed by IASI

C. Scannell et al.

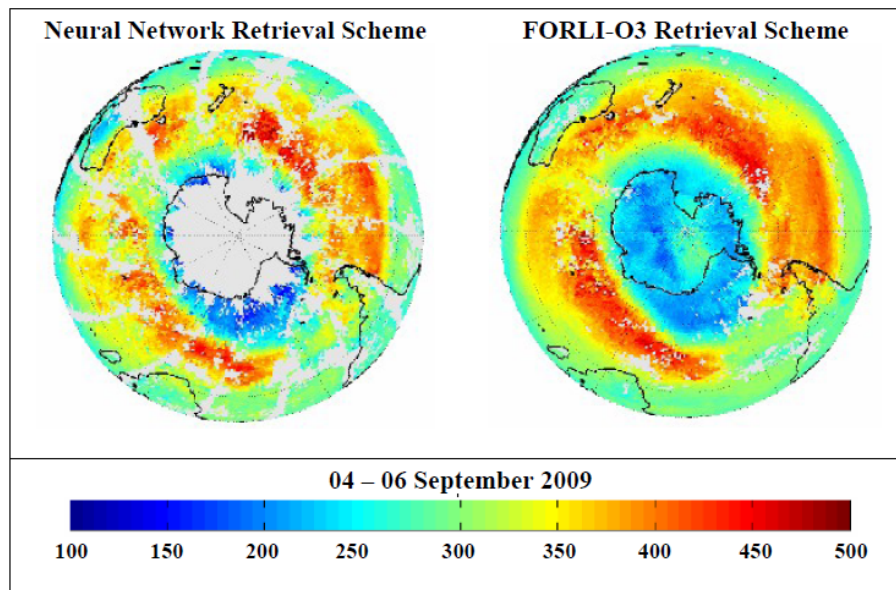


Fig. 2. Antarctic projections of IASI total ozone column distribution retrieved from the Neural Network scheme (left) and the FORLI-O3 scheme (right). Data are averaged over a $1^\circ \times 1^\circ$ grid over 3 days from 4 to 6 September.

[Title Page](#)[Abstract](#)[Introduction](#)[Conclusions](#)[References](#)[Tables](#)[Figures](#)[⏪](#)[⏩](#)[◀](#)[▶](#)[Back](#)[Close](#)[Full Screen / Esc](#)[Printer-friendly Version](#)[Interactive Discussion](#)

A review of the ozone hole from 2008 to 2010 as observed by IASI

C. Scannell et al.

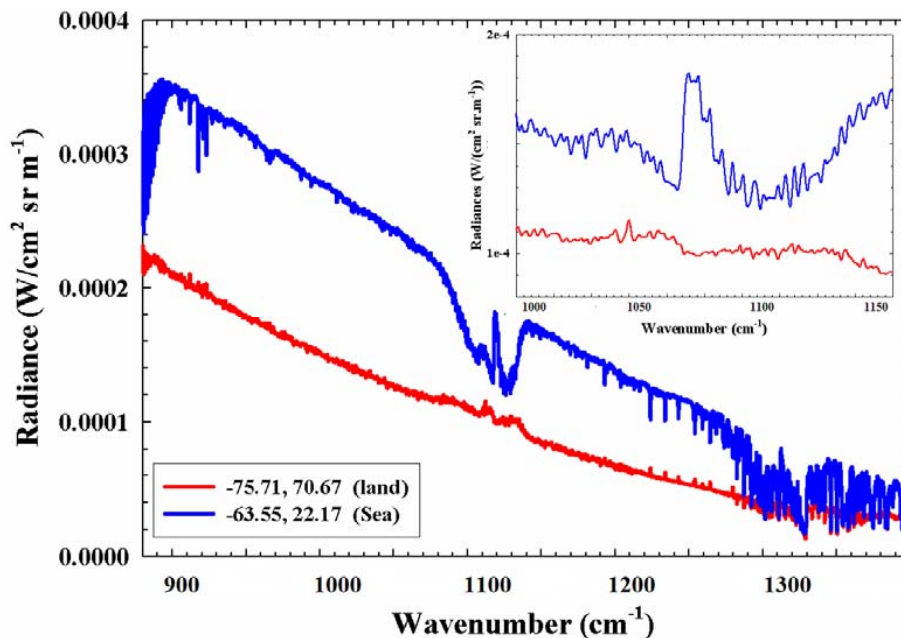


Fig. 3. Illustration of two spectra in radiances, taken over the Antarctic. The blue spectrum is representative of spectra over the ocean close to the Antarctic and the red spectrum is representative of those taken over the Antarctic continent itself. Inset into the figure are the same spectra but focused on the area of the spectra in which ozone absorbs. See Fig. 4 for the location of both measurements.

[Title Page](#)[Abstract](#)[Introduction](#)[Conclusions](#)[References](#)[Tables](#)[Figures](#)[⏪](#)[⏩](#)[◀](#)[▶](#)[Back](#)[Close](#)[Full Screen / Esc](#)[Printer-friendly Version](#)[Interactive Discussion](#)

A review of the ozone hole from 2008 to 2010 as observed by IASI

C. Scannell et al.

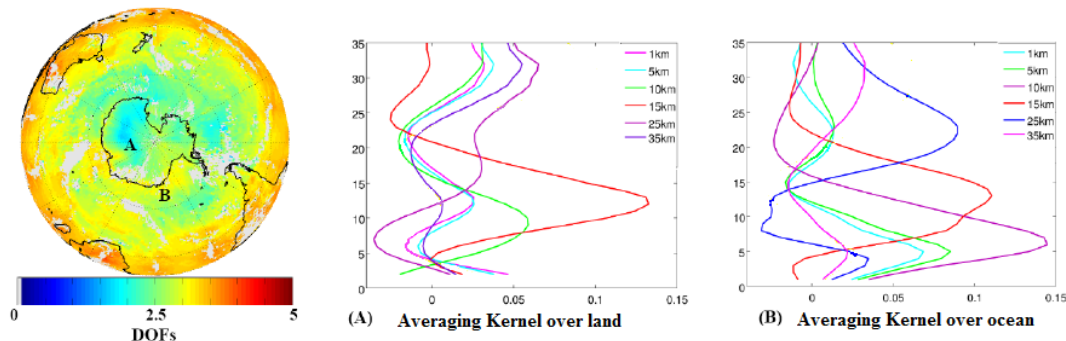


Fig. 4. Left panel: Antarctic projection of the IASI DOFs distribution. Middle and right panel: Averaging kernel functions for different altitudes in partial columns characterizing the retrievals over the land **(A)** and over the ocean **(B)** respectively (shown in Fig. 3). It highlights the difficulties in retrieving over the Antarctic region. The averaging kernels of a retrieval over ice can often be less defined than those over the ocean due to emissivity and poor thermal contrast as shown in this figure.

Title Page

Abstract

Introduction

Conclusions

References

Tables

Figures

⏪

⏩

◀

▶

Back

Close

Full Screen / Esc

Printer-friendly Version

Interactive Discussion

A review of the ozone hole from 2008 to 2010 as observed by IASI

C. Scannell et al.

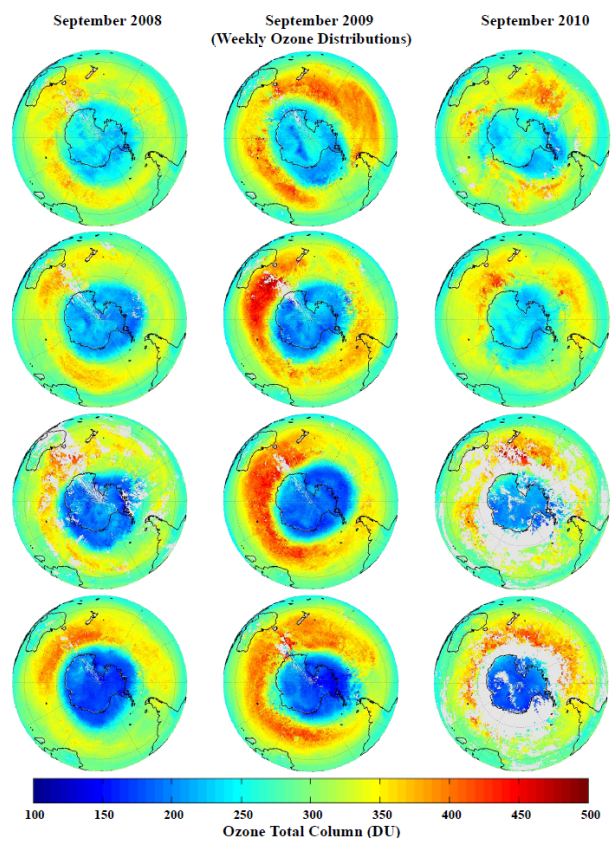


Fig. 5. Antarctic projection of IASI total ozone columns (DU) retrieved from the FORLI-O3 algorithm. Data are averaged over a $1^\circ \times 1^\circ$ grid and over each week of the peak month (September) during the ozone hole period for 2008, 2009 and 2010. For the two last weeks of September 2010 the data are more sparse because part of the L2 temperature data was not provided by EUMETSAT.

Title Page

Abstract	Introduction
Conclusions	References
Tables	Figures

◀
▶

◀
▶

Back	Close
------	-------

Full Screen / Esc

Printer-friendly Version

Interactive Discussion



A review of the ozone hole from 2008 to 2010 as observed by IASI

C. Scannell et al.

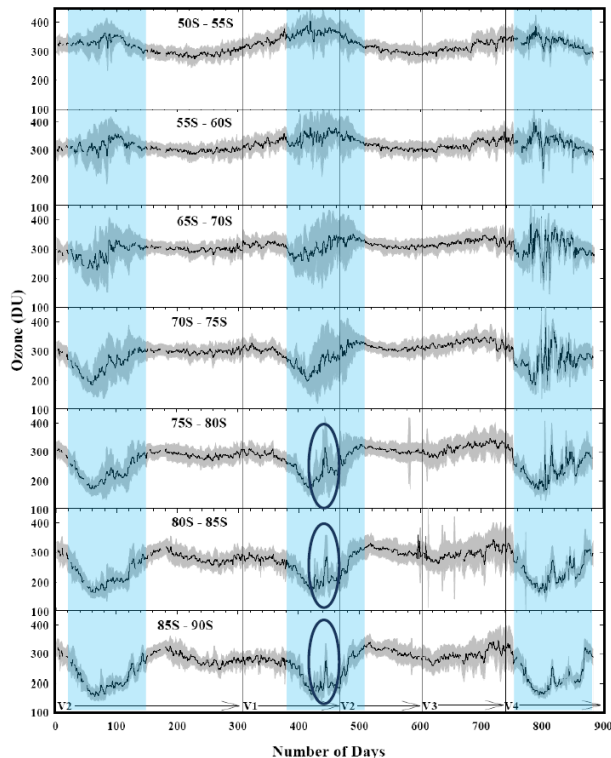


Fig. 6. Daily time series from the beginning of August 2008 to the end of December 2010 showing the evolution of the ozone concentration in DU for each day at 5° latitude increments from 50° S to 90° S. The daily measurements are described by the black line, the shaded grey represents the standard deviation about the average and the shaded blue area represents the ozone hole period. Version 1, 2, 3 and 4 (V1, V2, V3 and V4 respectively) are different versions of the FORLI-O3 program, numbered according to the date there were implemented (vertical lines). The arrows show the data generated using each version. The circled areas highlight some inter-annual variability which is discussed in the text.

Title Page

Abstract

Introduction

Conclusions

References

Tables

Figures

◀

▶

◀

▶

Back

Close

Full Screen / Esc

Printer-friendly Version

Interactive Discussion

A review of the ozone hole from 2008 to 2010 as observed by IASI

C. Scannell et al.

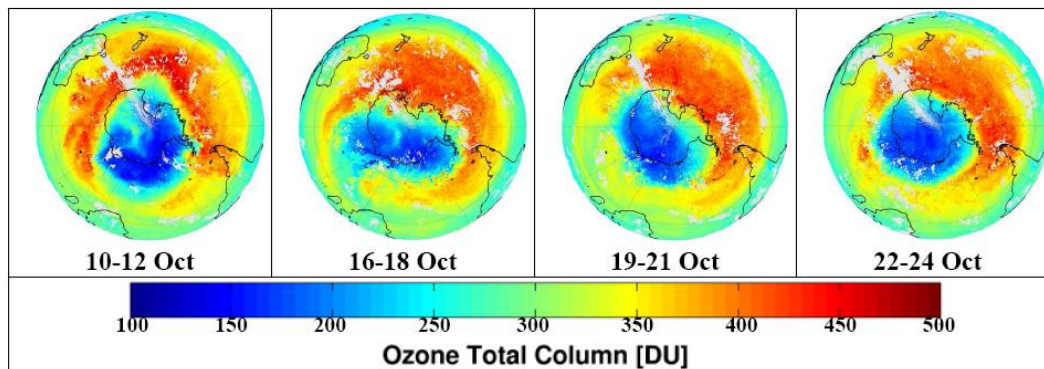


Fig. 7. Antarctic projections of the total ozone column distributions averaged over 3 day periods in October 2009. The change from a circular to elliptical rotation and back again is clearly visible from the distributions. Data are averaged over a $1^\circ \times 1^\circ$ grid.

[Title Page](#)[Abstract](#)[Introduction](#)[Conclusions](#)[References](#)[Tables](#)[Figures](#)[◀](#)[▶](#)[◀](#)[▶](#)[Back](#)[Close](#)[Full Screen / Esc](#)[Printer-friendly Version](#)[Interactive Discussion](#)

A review of the ozone hole from 2008 to 2010 as observed by IASI

C. Scannell et al.

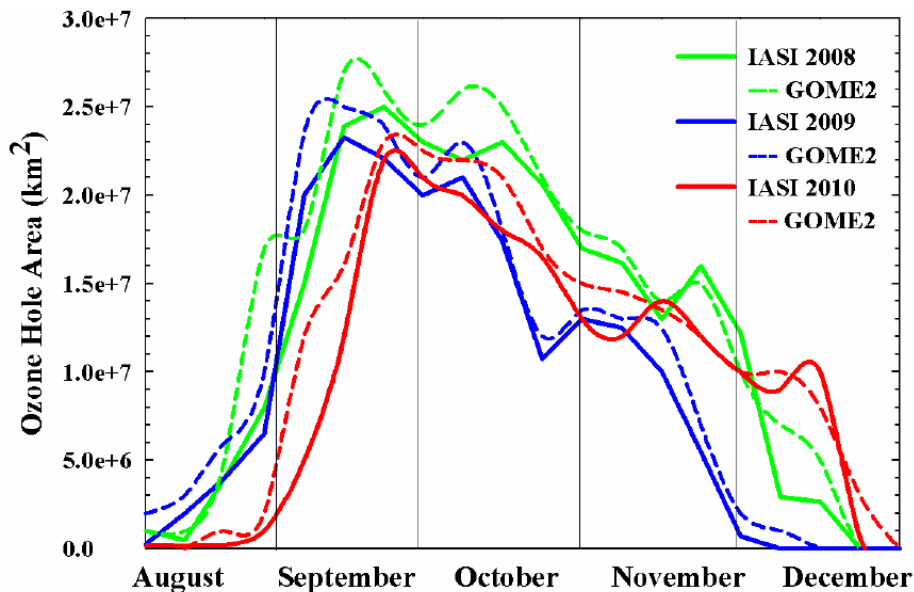


Fig. 8. Temporal evolution of the area of the ozone hole (defined as lower than 220 DU) as measured from IASI (solid line) and GOME-2 (dashed line) for 2008 (green), 2009 (blue) and 2010 (red). This data set is compiled from weekly averaged data from a $1^\circ \times 1^\circ$ resolution dataset.

[Title Page](#)[Abstract](#)[Introduction](#)[Conclusions](#)[References](#)[Tables](#)[Figures](#)[◀](#)[▶](#)[◀](#)[▶](#)[Back](#)[Close](#)[Full Screen / Esc](#)[Printer-friendly Version](#)[Interactive Discussion](#)

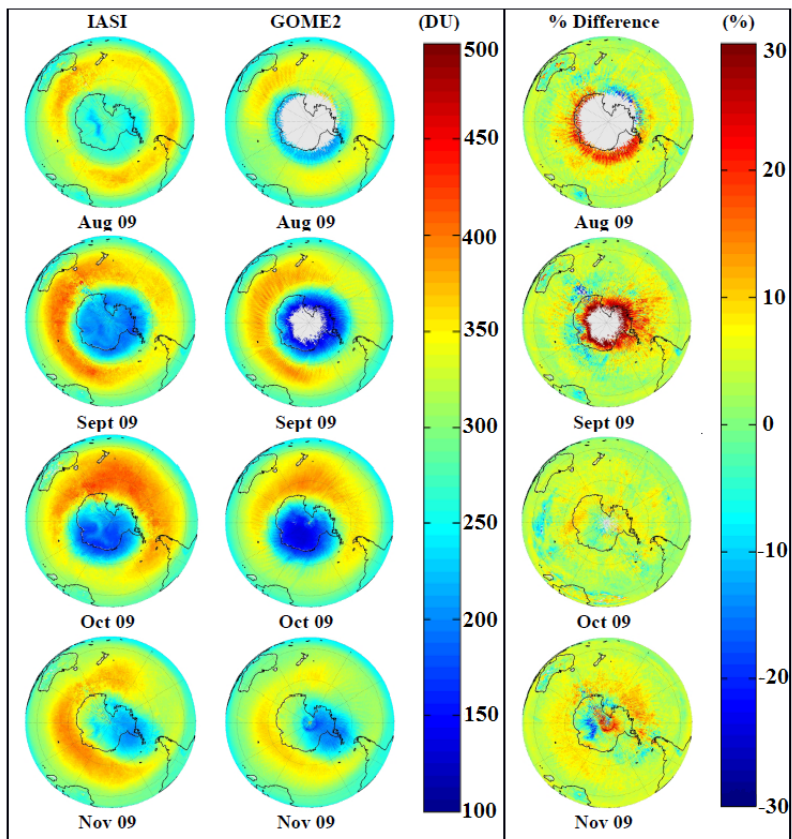


Fig. 9. Antarctic projections of IASI and GOME2 total ozone column monthly averaged distribution for the ozone hole period of 2009 along with the percentage difference between both instruments. One of the key strengths of the IASI mission is the ability of IASI to measure continually during the polar night, which is not always the case with UV-vis instruments such as GOME-2 which have to fill in data gaps with assimilated data.

A review of the ozone hole from 2008 to 2010 as observed by IASI

C. Scannell et al.

Title Page

Abstract Introduction

Conclusions References

Tables Figures

◀ ▶

◀ ▶

Back Close

Full Screen / Esc

Printer-friendly Version

Interactive Discussion



A review of the ozone hole from 2008 to 2010 as observed by IASI

C. Scannell et al.

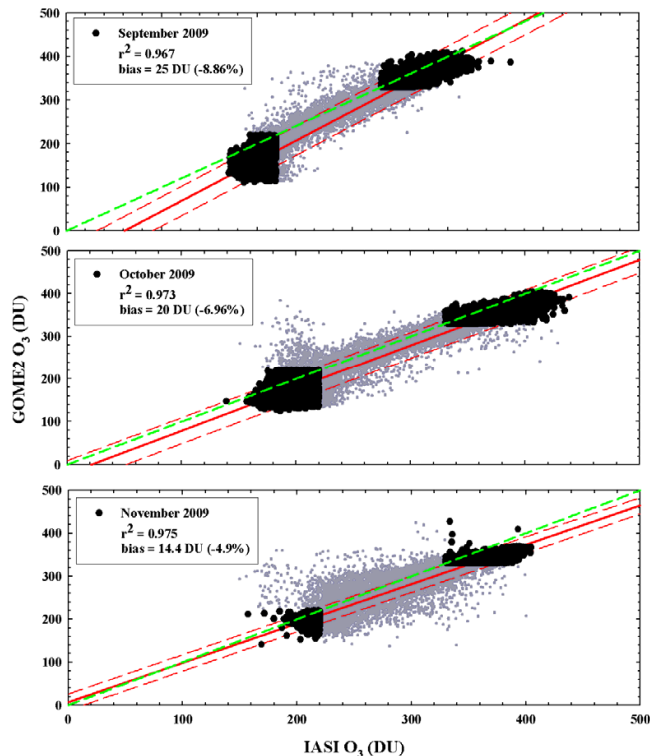


Fig. 10. Correlation between GOME-2 and IASI for September (top panel), October (middle panel) and November (bottom panel) of 2009 for the ozone hole (ozone values less than 220 DU) and the ozone hole vortex (ozone values greater than 320 DU). The black data below 220 DU and above 320 DU represent ozone values within the ozone hole and in its associated vortex respectively. The grey data represents all other data south of 45° S, the area for which the ozone hole is defined, which do not lie within the hole or vortex regions. The linear regressions (solid red line), confidence intervals (dashed red lines) and 1:1 ratios (dashed green line) are also represented. The average bias is also presented.

Title Page

Abstract

Introduction

Conclusions

References

Tables

Figures

◀

▶

◀

▶

Back

Close

Full Screen / Esc

Printer-friendly Version

Interactive Discussion

A review of the ozone hole from 2008 to 2010 as observed by IASI

C. Scannell et al.

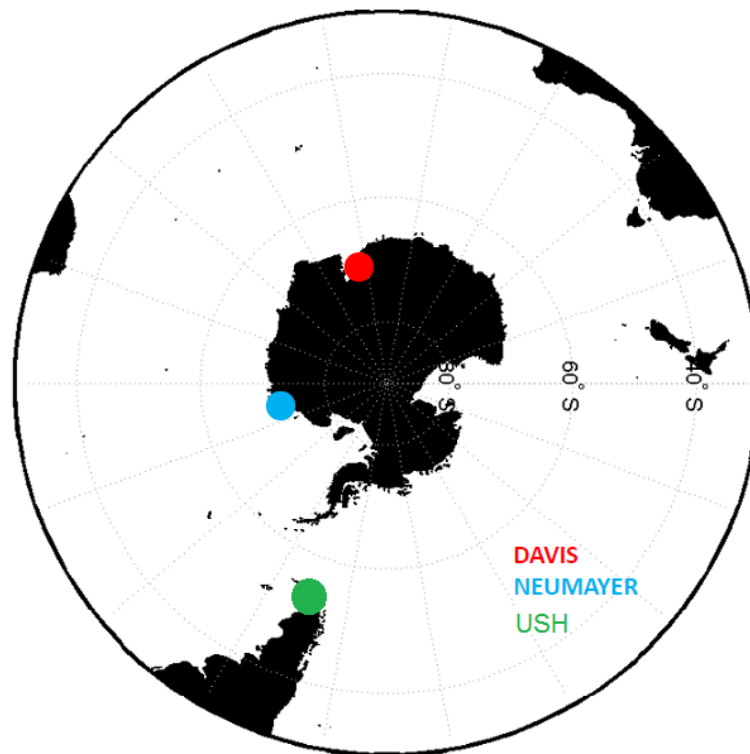


Fig. 11. Geographic locations of the three ground based stations used for the IASI/ozone sonde profile comparison; Davis in red, Neumayer in blue and USH in yellow. The stations chosen represent locations inside the ozone hole (Davis and Neumayer) and in the associated vortex (Davis and USH).

[Title Page](#)[Abstract](#)[Introduction](#)[Conclusions](#)[References](#)[Tables](#)[Figures](#)[◀](#)[▶](#)[◀](#)[▶](#)[Back](#)[Close](#)[Full Screen / Esc](#)[Printer-friendly Version](#)[Interactive Discussion](#)

A review of the ozone hole from 2008 to 2010 as observed by IASI

C. Scannell et al.

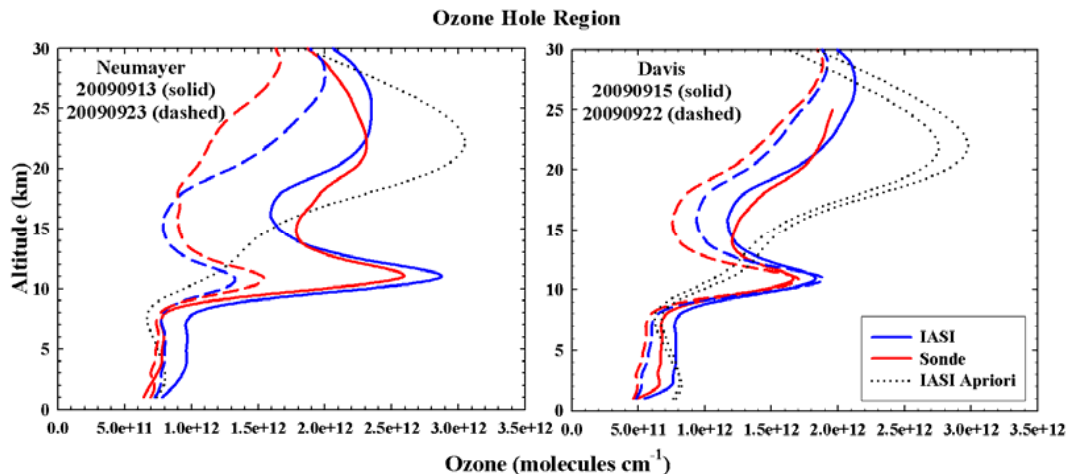


Fig. 12. Comparisons between IASI and ozone sonde profiles measured within the ozone hole at the Neumayer (left panel) and Davis (right panel) stations for different days of September 2009. The IASI a priori is represented by the black dotted line. The IASI profile is an averaged profile of a number of profiles co-located in time and space to the ozone sonde measurements. The ozone sonde profile has been convolved with the IASI averaging kernels. Note that the a priori profile here has been converted from mixing ratios (independent of temperature and pressure) to density (dependent on temperature and pressure). Thus if temperature and pressure change from one location or day to another, different a priori profiles in density will be found (as is the case in Fig. 12, right panel).

[Title Page](#)
[Abstract](#)
[Introduction](#)
[Conclusions](#)
[References](#)
[Tables](#)
[Figures](#)
[◀](#)
[▶](#)
[◀](#)
[▶](#)
[Back](#)
[Close](#)
[Full Screen / Esc](#)
[Printer-friendly Version](#)
[Interactive Discussion](#)

A review of the ozone hole from 2008 to 2010 as observed by IASI

C. Scannell et al.

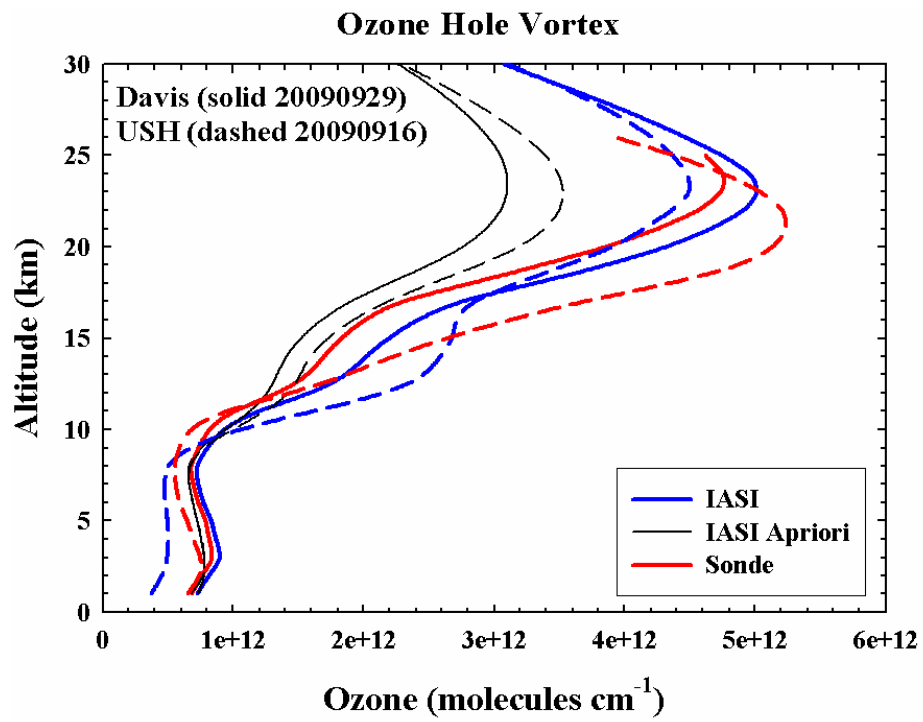


Fig. 13. Comparison between IASI and ozone sonde profiles measured within the ozone hole vortex region at the Davis (left panel) and USH (right panel) stations for different days in September 2009. The IASI a priori is represented by the black dotted line. The IASI profile is an averaged profile of a number of profiles co-located in time and space to the ozone sonde measurements. The ozone sonde profile here has been convolved with the IASI averaging kernels.

Title Page

Abstract Introduction

Conclusions References

Tables Figures

⏪ ⏩

◀ ▶

Back Close

Full Screen / Esc

Printer-friendly Version

Interactive Discussion

